Title: Effects of 4-Nonylphenol on spermatogenesis and induction of testicular apoptosis through oxidative stress-related pathways

Author: Peng Duan Chunhui Hu Holly J. Butler Chao Quan Wei Chen Wenting Huang Sha Tang Wei Zhou Meng Yuan Yuqin Shi Francis L. Martin Kedi Yang

PII: S0890-6238(16)30066-1
DOI: http://dx.doi.org/doi:10.1016/j.reprotox.2016.04.016
Reference: RTX 7279

To appear in: *Reproductive Toxicology*

Received date: 31-10-2015
Revised date: 16-4-2016
Accepted date: 19-4-2016

Please cite this article as: Duan Peng, Hu Chunhui, Butler Holly J, Quan Chao, Chen Wei, Huang Wenting, Tang Sha, Zhou Wei, Yuan Meng, Shi Yuqin, Martin Francis L, Yang Kedi.Effects of 4-Nonylphenol on spermatogenesis and induction of testicular apoptosis through oxidative stress-related pathways.*Reproductive Toxicology* http://dx.doi.org/10.1016/j.reprotox.2016.04.016

Title Page

The title of the paper

Effects of 4-Nonylphenol on spermatogenesis and induction of testicular apoptosis through oxidative stress-related pathways

The full names of the authors

Peng Duan[a], Chunhui Hu[b], Holly J. Butler[c], Chao Quan[a], Wei Chen[a], Wenting Huang[a], Sha Tang[a], Wei Zhou[a], Meng Yuan[a], Yuqin Shi[d] , Francis L. Martin[c] & Kedi Yang *[a]

Affiliations of authors

[a]*MOE (Ministry of Education) key lab of Environment and Health, Department of Occupational and Environmental Health, Tongji Medical College, Huazhong University of Science and Technology, Wuhan 430030, China;*

[b]*Department of Laboratory Medicine, Taihe Hospital, Hubei University of Medicine, Shiyan 442000, Hubei, China;*

[c]*Centre for Biophotonics, Lancaster Environment Centre, Lancaster University, Bailrigg, Lancaster LA1 4YQ, UK;*

[d]*Department of epidemiology and health statistics, School of Public Health, Medical College, Wuhan University of Science and Technology, Wuhan 430030, China*

Correspondence to: *Kedi Yang*; *e-mail: yangkd@mails.tjmu.edu.cn*; *Tel: +86-0278-3693897; Fax: +86-0278-3657765*

Research highlights

► *Exposure to 4-Nonylphenol induced hormetic dose-dependent changes in testicular structure and sperm parameters.*

► *High-dose exposure of Sprague-Dawley rats to 4-Nonylphenol exerted adverse effects on the male reproductive development and function.*

► *Subacute exposure to 4-Nonylphenol caused oxidative stress in testis and activated the p53-Bcl-2/Bax and -Fas/FasL pathways, resulting in testicular apoptosis.*

ABSTRACT

This study tested the hypothesis that prepubertal exposure to 4-Nonylphenol (NP) affects reproductive function in male rats. Twenty-four rats at five-weeks-old were randomly divided into four groups and treated with NP at varying concentrations (0, 5, 20, and 60 mg/kg/2d) for thirty days by intra-peritoneal injection. 60 mg/kg NP induced spermatogenic degeneration and pronounced deficits in epididymal sperm count, motility and function, whereas potentially stimulatory effects were observed at 5 NP mg/kg. Moreover, 60 mg/kg NP resulted in a significant reduction in fructose, FSH and LH; induced apoptosis related to oxidative stress; inhibited mRNA and protein levels of Bcl-2 and PCNA; as well as the additional up-regulation of p53, Bax, Apaf-1, cytochrome *c*, cleaved-caspase-3, Fas and FasL expression. Our data suggest potentially hormetic effects of NP on spermatogenic function. High-dose NP impairs testicular development and function by reducing cell proliferation and inducing apoptosis involving oxidative stress-related p53-Bcl-2/Bax and -Fas/FasL pathways.

Keywords:

4-Nonylphenol, Hormetic effect, Reproductive toxicity, Oxidative stress, Apoptosis, Intrinsic and extrinsic apoptotic pathways, Rats

1. Introduction

4-Nonylphenol (NP) has received increased international attention due to its widespread environmental occurrence, as it is known to disturb hormone functions and inhibit stimulation of the endocrine system [1]. NP has been detected in almost all environmental water matrices, including drinking water, and has been shown to have relatively high coefficients for adsorption onto sediment and soil [2]. Due to its lipophilic properties and long half-life, NP is ubiquitous in the food chain, including fish, animal tissues, milk, and cereals [3]. Due to the concerning environmental concentrations (surface water) and potential toxicity of NP, the chemical has been included in the list of 33 priority hazardous substances regulated by the European Parliament Directive 2008/105/EC [4].

The entry of NP into the biological system has attracted concern about reproductive and developmental disorders in human populations exposed to the affected food chain [2, 5]. To date, we are aware of only one epidemiological study; was an investigation conducted in China that addressed urinary NP level in relation to idiopathic male infertility [6]. The results of in vitro studies have suggested that exposure to NP negatively affects sperm motility and viability [7, 8].

Similarly, previous *in vivo* studies have demonstrated that NP exposure adversely impacts spermatogenic development and decreases sperm counts and motility [9, 10]; however, there have been no reports that describe the adverse effects of NP on epididymal sperm parameters in rats at prepubertal age. This stage is considered as one of highly sensitive periods to subtle effects of xenoestrogens exposure and thus the effects of NP need to be observed at this developmental time point [11, 12].

Oxidative stress (OS), which results from an imbalance between reactive oxygen species generation and antioxidant defences, has been linked to germ cell apoptosis and male infertility [13]. Previous studies unanimously supported that OS potentially interferes with normal spermatogenic process and sperm functionality in mammals [14, 15]. Interestingly, NP administration not only induces oxidative stress in the testis, but also triggers testicular apoptosis [15, 16]. Furthermore, Lu et al. reported that OS is involved in NP-mediated apoptosis in testicular germ cells *in vivo* [10]. OS is capable of inducing apoptosis that is largely dependent on caspase activities[17]. It is has been determined that caspase activation occurs through mitochondrial cytochrome *c*/Apaf-1 and Fas/FasL signalling pathways in vivo and in vitro[18]. We believe that further investigation regarding the apoptotic mechanism of NP-induced OS and the subsequent activation of extrinsic and intrinsic apoptosis signalling pathways are necessary to better understanding of the toxicological effects of NP.

In this study, male rats were treated with NP during the prepubertal period, followed by evaluation of epididymal sperm parameters and histopathological examination. Serum follicle-stimulating hormone (FSH), luteinizing hormone (LH), testosterone concentrations and the content of fructose in testis were evaluated. The in vivo antioxidant activity of NP and relative changes in anti-oxidative gene and pro-/anti- apoptotic gene mRNA expression were studied to reveal the underlying apoptotic mechanisms. We then investigated the potential role of NP in proliferation inhibition and apoptosis induction of the germ cells in the testis, and explored the NP-induced mitochondria-and death receptor-mediated apoptosis.

2. Materials and methods

2.1. Chemicals

4-Nonylphenol (Mixture of isomers; CAS no. 84852-15-3; empirical formula $C_{15}H_{24}O$; molecular weight 220.35) with 99% analytical standard was purchased from ACROS Organics (Leicestershire, UK). DeadEnd™ Fluorometric TUNEL System kit was purchased from Promega (Madison, WI, USA). Mouse monoclonal proliferating cell nuclear antigen (PCNA) antibody and p53 were purchased from Abcam Inc. (Cambridge, MA, USA). FSH immunoradiometric assay (IRMA) kits and LH radioimmunoassay (RIA) kits were purchased from MP Biochemicals (Asse-Relegem, Belgium). BCA protein assay kit and RIPA lysis buffer were purchased from the Beyotime Company of Biotechnology (Shanghai, China). The fructose assay kit, malondialdehyde (MDA), glutathione peroxidase (GSH-Px) and superoxide dismutase (SOD) kits were obtained from Nanjing Jiancheng Bioengineering Institute (Nanjing, China). TRIzol® Reagent and Platinum® SYBR® Green qPCR SuperMix-UDG kit purchased from Invitrogen (Carlsbad, CA). Revert Aid First Strand cDNA Synthesis kit was purchased from Fermentas UAB (Vilnius, Lithuania). Rabbit monoclonal antibody against pro-caspase-3 was purchased from Santa Cruz Biotechnology (Santa Cruz, CA, USA). Rabbit monoclonal antibodies against p53, Bcl-2, PCNA,

Bax, Apaf-1, cytochrome *c*, cleaved-caspase-3, Fas, FasL and TNF-α were purchased from Cell Signalling Technology (Cambridge, MA, USA). Goat anti-rabbit and anti-mouse secondary antibodies were purchased from Amersham (Buckinghamshire, UK).

2.2. Animals and treatment

All animal experimental procedures were carried out in accordance with the Guide for the Care and Use of Laboratory Animals published by Ministry of Health of People's Republic of China. The experimental protocols were approved by the Institutional Animal Care and Use Committee of Tongji Medical College (Wuhan, China).

Twenty-four Sprague-Dawley (SD) rats, clean-grade healthy, male, 4 weeks old, weighing 140-160 g, were purchased from Tongji Medical College Animal Centre (Wuhan, China), and were housed in an animal room where the temperature (22-25°C) and relative humidity (45-60%) were controlled. A 12-h day-night cycle was maintained for the lighting period. Rats had free access to purified water and animal feed.

After a week of acclimatisation, 5-week-old rats were randomly allocated into four groups (n = 6): three NP treatment groups (5, 20 and 60 mg/kg body weight/two days) and a control group. Rats were exposed to different doses of NP dissolved in corn oil by intraperitoneal injection for 30 consecutive days to cover the spermatogenic cycle according to Yu et al. [19]. The injection volume of each dose was 10 mL/kg body weight and rats were weighed immediately prior to treatment to calculate the actual volume of administration. The control rats received the same volume of corn oil vehicle.

2.3. Collection of blood and testis samples

After treatment, six rats in each group were weighed accurately. Rat blood samples were collected from the eye vein by removing the eyeball quickly. Then the rats were sacrificed by decapitation, and their testis were dissected out immediately, trimmed off the attached tissues and weighed on the ice plate. The blood was allowed to coagulate for 2 h at 4°C and then centrifuged at 3000 rpm for 10 minutes. Serum was separated and stored at -20°C until biochemical analysis. The tissue (5×5×3 mm) cut from the left testis was fixed with 4% paraformaldehyde buffer, processed, embedded in paraffin for haematoxylin-eosin (H&E) staining, terminal deoxynucleotidyl transferase-mediated nick and labelling (TUNEL) analysis and immunohistochemistry. The tissue (2×2×2 mm) cut from the right testis was fixed in 2.5% glutaraldehyde for electron microscopic observations. The rest of the tissue of the bilateral testis was frozen by immersion in liquid nitrogen and stored at -80°C until biochemical analysis.

2.4. Detection of semen parameters

The left epididymis was used for evaluation of sperm parameters. After decapitation, cauda epididymis and ductus deferens were dissected out immediately, trimmed off the attached tissues. Then, the left epididymis of each rat rinsed briefly in pre-warmed physiological saline (37°C) and then placed in a small petri dish with 2 mL sperm nutrient solution (0.35 g/L NaHCO3, 4.2 g/L HEPES, 2.0 g/L BSA, 0.35 g/L $NaHCO_3$, 0.1 g/L sodium pyruvate, 0.9 g/L D-glucose, and 0.025 g/L soybean trypsin inhibitor in Hanks balanced salt solution, pH=7.4, 37°C). Ten deep cuts were made along the proximal and distal cauda of epididymis to release the sperm and stored in a CO_2

incubator (humidified atmosphere of 95% air, 5% CO_2, 37°C) for 5 minutes. Following this, a sperm suspension (5µl) was applied onto a clean glass slide and computer-assisted semen analysis was used to detect sperm count, motility and motion parameters, as previously described [20]. The control data are consistent with normal historical control data for this lab.

2.5 Determination of sperm malformation rate

The right epididymis was used for routine sperm deformation test. Sperm suspension taken from the right epididymis from each rat was prepared as described above (Section 2.4). A drop of the suspension was placed on a clean slide and smeared evenly, after which the smears were air dried, fixed with 1% paraformaldehyde, and then stained with 2% eosin for 2 h. The slides were washed in water and air dried again. Under the microscope, 400 sperm were observed per rat. The percentage of abnormal sperm was recorded.

2.6. Estimation of fructose and hormone levels

The serum was stored at -80°C was thawed. Serum hormone concentrations were measured by double-antibody ELISA methods using LH, FSH and T RIA kits according to the standard protocol supplied by the kit manufacturer. The content of fructose and protein in the testis were determined according to the methods described in the references using commercial kits. All samples and standards were run in triplicate.

2.7. Testicular Histopathology

The tissues were embedded in paraffin. Then 4-µm sections were cut and stained with HE, and examined under a fluorescence microscope (Olympus, Tokoy, Japan) according to standard protocols.

2.8. Assay of oxidative biochemical parameters

OS markers including MDA, SOD and GSH-Px were detected in both plasma and testis samples. Notably, testicular tissues were homogenised in RIPA lysis buffer. The protein content of testicular homogenate supernatant was quantified via BCA protein content assay. The levels of MDA and the activities of SOD and GSH-Px were determined using commercial kits. All assays were performed according to the instructions of the manufacturer.

2.9. Transmission electron microscopy (TEM)

After being fixed in 2.5% glutaraldehyde, small testicular specimens were post-fixed for 2 h with 1% osmium tetroxide, dehydrated and then embedded in Eponate-12 overnight. Finally, ultrathin sections were stained with 1% uranyl acetate and 1% lead citrate. The ultrastructural features of germ cells were examined and photographed using a Tecnai G2 12 Transmission electron microscopy (FEI Company, Holland). This experiment was repeated twice.

2.1.1. TUNEL staining and quantitative analysis

Germ cell apoptosis was evaluated by the terminal deoxyribonucleotidyl transferase (TDT)-mediated dUTP-digoxigenin nick end labeling (TUNEL) assay. To detect nuclei with DNA fragmentation, representing a hallmark of apoptosis, paraffin-embedded sections (4-µm thick) were stained by using the DeadEnd™ Fluorometric TUNEL System kit. After adding DAPI nuclear stain in mounting medium, images were examined by the fluorescence microscope to

detect localised green fluorescence of apoptotic cells. Two testicular cross-section slides from each rat were used for the quantitative study. Apoptotic index was calculated [100%×(number of TUNEL-positive nuclei/total number of nuclei)]. The result was regarded as the mean of six different seminiferous tubules on each section. The image was captured with a colour video camera.

2.1.2. Cell proliferation assay and localization of p53 by immunohistochemistry

Paraffin wax tissue sections of 4-µm thickness were deparaffinised and rehydrated. Endogenous peroxide activity was inhibited by incubating sections in 0.3% hydrogen peroxide/methanol for 30 minutes. Sections were then incubated overnight at 4°C with mouse monoclonal anti-PCNA (1:200 dilution) and anti-p53 (1:500 dilution), respectively. A secondary anti-mouse antibody (1:500) was then applied to each slide, followed by incubation with streptavidin horseradish peroxidase enzyme conjugate. Immunoreaction products were stained with using 3,3′-diaminobenzidine as a chromogen. Each slide was counterstained with Mayer′s haematoxylin. Negative controls were prepared with the sections stained without the primary antibody. For each section, six seminiferous tubules were counted for the total number of nuclei versus nuclei positively stained in brown. The percentage of PCNA-positive cells was calculated as follows: (number of PCNA-positive cells)/(total number of cells within the tubule)×100. The immunohistochemical expression of active p53 was examined and photographed under a fluorescence microscope. These analyses were performed in two sections from each rat.

2.1.3. Real-Time Quantitative PCR

Real-time (RT) PCR was performed to quantify gene expression following the method of Quan et al. [20]. Briefly, total RNA was extracted with Trizol reagents according to the manufacturer's protocol. Primer sequences used for real-time RT-PCR analysis are summarised in Table S1. Equal amounts of RNA (2 µg) was reverse-transcribed into complementary DNA using Revert Aid First Strand cDNA Synthesis Kit. Afterwards, RT-PCR was performed with an ABIPRISM® 7900HT Sequence Detection System (Applied Biosystems) using Platinum® SYBR® Green qPCR SuperMix-UDG with ROX. β-actin was regarded as a housekeeping gene. The results were represented as a ratio: targeted gene/β-actin mRNA.

2.1.4. Protein extraction and Immunoblotting

After the indicated treatment, SCs were harvested and washed twice with ice-cold phosphate-buffered saline and lysed in lysing buffer. Protein content was quantified using a BCA protein assay kit, and lysate containing 20–50 µg of protein was subjected to SDS-polyacrylamide gel and then transferred electrophoretically onto a nitrocellulose membrane followed by Western blot analyses as described previously [21]. The immune-reactive protein bands were visualised using the enhanced chemiluminescence plus Western blot detection system. Densitometric analysis was performed on scanned images of blots using the Gel-Pro Analyzer 4.0 software.

2.1.5. Statistical Analysis.

All statistical calculations were performed using the SPSS statistical package 12.0 (SPSS Inc., Chicago, IL, USA). Quantitative results were expressed as mean ± standard deviation (SD) of at least three independent experiments. Statistical significance between three or more groups was

performed by the one-way analysis of variance (ANOVA). Student-Newman-Keuls (SNK) test was used to determine significant differences between treated and control groups. We considered values of $P<0.05$ to be statistically significant.

3. Results

3.1. General observation

No deaths were observed in any group. No significant difference was observed in the initial body weights, terminal body weights, body weight gain or the weight coefficient of testis among the four groups ($P>0.05$, data not shown).

3.2. Evaluation of testicular sperm counts and motility

Data from computer-assisted sperm analysis are shown in Table 1. When rats were treated with the 60 mg/kg NP, significant decreases ($p<0.05$) in total sperm counts, motility and motile density were observed in comparison with the control group. In contrast, marked increases in total counts, motility and motile density were observed in rats treated with the 5 mg/kg NP ($p<0.05$). Accordingly, there was a statistically significant difference ($p<0.01$) between the 5 mg/kg and 60 mg/kg groups.

Regarding the motility parameters, except for a significant decrease in the density of FP detected at NP 60, no alterations of other motility parameters such as curvilinear velocity (VCL), straight line velocity (VSL) and average path velocity (VAP) were found in the 60 mg/kg group when compared with the 0 mg/kg group. Notably, the density of sperm with forward progression (FP) was significantly elevated ($p<0.05$) in rats treated with 5 mg/kg NP compared with the 0 mg/kg group. However, the VCL, maximal amplitude of lateral head displacement (ALH) and the density of FP in the 60 mg/kg group were much lower than those in the 5 mg/kg group ($p<0.05$).

3.3. Effect of NP on rat sperm quality

Compared with the 0 mg/kg group, the percentages of B, C, D and C&D grade motile sperm did not reveal any significant alterations after exposure to 5 mg/kg NP, but there was a significant increase in sperm of grade A and A&B ($p<0.05$, Table 1). The percentage of A&B grade sperm tended to decrease in the 60 mg/kg group when compared with the 0 mg/kg group, but there was no significant difference between the two groups ($p>0.05$).

3.4. The frequency of abnormal spermatozoa

As shown in Fig. 1, the changes in epididymal sperm characteristics were observed in response to NP treatment. Five different abnormalities in sperm morphology were found: coiled and bent tail, tailless form, double head, pin head and big head. The 5 mg/kg and 0 mg/kg NP-treated groups did not differ significantly in terms of their percentage of total sperm abnormalities, but the 20 mg/kg and 60 mg/kg NP-treated rats had significantly higher abnormal sperm morphology rates than the 0 mg/kg group ($p<0.05$; Table 1).

3.5. Effects on reproductive hormones and fructose

The plasma levels of FSH and LH were reduced in a dose-dependent manner, and there was a

significant difference (p<0.05) between the 0 mg/kg and 60 mg/kg groups (Fig. 2). In the 60 mg/kg group, the plasma testosterone levels did not significantly change compared to the 0 mg/kg group (Fig. 2). The fructose level dramatically dropped in rats treated with the 60 mg/kg NP when compared with the control (p<0.05; Fig. 2).

3.6. NP-induced testicular histopathological changes

NP also induced histological alterations in the testis (Fig. 3). The 0 mg/kg group showed all of the successive stages of spermatogenesis, and a compact and a regular arrangement of cells in the seminiferous tubules (Fig. 3A). The rats exposed to NP at 5 mg/kg did not exhibit histological differences compared to the control (Fig. 3B); whilst abundant sperm could be detected in the lumen of the seminiferous tubules. Exposure of the rats to 20 and 60 mg/kg NP provoked severe seminiferous tubule destruction, namely the spermatogenesis spermatogenesis derangement, spermatogenic cell sloughing and the vacuolization of the seminiferous tubular cells (Fig. 3C and D), particularly in the 60 mg/kg group.

3.7. Role of NP on OS

Testis from rats in the 60 mg/kg group showed a significant depletion in SOD and GSH-Px activity (p<0.05), while the level of MDA was increased (p<0.05) when compared with the controls (Fig. 4A). Similarly, when compared with the control, NP-treated rats at NP 20 and 60 mg/kg showed a marked decline (p<0.05) in serum SOD and GSH-Px activity and a pronounced increase (p<0.05) in the MDA content (Fig. 4B). Furthermore, the mRNA levels of CAT, GPx1, SOD1 and CYP1B1 were significantly lower at NP 60 (p<0.05, Fig. 5).

3.8. Ultrastructural Observations

The TEM examination revealed that seminiferous tubule basement membrane in the 0 mg/kg group was smooth and compact; spermatocytes appeared normal; and endoplasmic reticulum and mitochondria were evenly distributed into the cytoplasm (Fig. 6A). The rat testis at NP 5 mg/kg did not show any obvious ultrastructural change when compared to the 0 mg/kg group. However, in the 20 mg/kg group, more intracellular vacuoles and lipid droplets were present; the nucleus had irregular nuclear membrane and abnormal distribution of heterochromatin; mitochondria were swollen, and the endoplasmic reticulum was expanded. At NP 60 mg/kg, germ cells with cellular fragmentation similar to apoptosis, disruption of cellular junctions and condensed nucleus were observed; the number of mitochondria and the amount of endoplasmic reticulum was decreased; and some of nucleolus and nuclear membrane even disappeared.

3.9. Effects of NP on the Apoptosis and Proliferation of Spermatogenic Cells

Higher-dose NP increased apoptotic testicular cells, detected with TUNEL staining (Fig. 6B), from 7.2±2.4% (20 mg/kg) to 8.5±1.9% (60 mg/kg). Compared with controls (1.03±0.25%), TUNEL-positive cells were considerably elevated by NP treatment (20 and 60 mg/kg) (p<0.01). Conversely, the percentages of PCNA-positive cells in the 20 and 60 mg/kg NP-treated group (72.55±9.36% and 54.36±8.33%, respectively) were statistically lower than in controls (88.62±7.25%) (p<0.05, Fig. 7A). Moreover, RT-PCR analysis revealed that NP treatment (20 and 60 mg/kg) significantly decreased the PCNA1 mRNA level compared with the control (p<0.01, Table 2). Interestingly, PCNA-positive cells were more abundant in the 5 mg/kg group

(92.74±10.52%) than the control, meanwhile, the PCNA1 mRNA level markedly up-regulated in the 5 mg/kg group (p<0.01).

3.1.1. Apoptosis and inflammatory-related mRNAs expression

As shown in Table 2, in the 60mg/kg NP-treated rats, compared to the control rats, the level of caspase-3 mRNA was significantly increased (p<0.05), while the expression level of caspase-7 was visibly decreased (p<0.01). Significant decreases in mRNA expression levels of anti-apoptotic Bcl-xl and Bcl-2 were observed in the 20 mg/kg group compared with those in the 0 mg/kg group, whereas NP (60 mg/kg) significantly up-regulated the pro-apoptotic Bax at mRNA levels (p<0.05). Furthermore, an obvious increase in the intensity of p53 expression was observed at NP 20 and 60 mg/kg (Fig. 7B). RT-PCR analysis confirmed a significant increase in mRNA levels of apoptotic genes including p53, cytochrome c, Apaf-1, Fas and FasL in the 60 mg/kg group (all p<0.05), compared to the control group. There were also significant differences observed between the 0 mg/kg and 60 mg/kg groups regarding the mRNA expression of inflammatory IL-1β, TNF-α and IFN-γ (all p<0.05). Surprisingly, caspase-1, -3, -6, -9 and IFN-γ mRNA expression was significantly decreased in the 5 mg/kg group in comparison with the control group (all p<0.05).

3.1.2. Western Blot Analysis

Consistent with the results above, the protein levels of Bcl-2, PCNA and pro-caspase-3 significantly decreased after treatment with NP (60 mg/kg) as shown by Western blot (Fig. 8A) and the quantification analysis (Fig. 8B, C and D). Moreover, the expression of p53, Bax, Apaf-1, cytochrome *c* and cleaved-caspase-3 was dramatically up-regulated at NP 60 (all p<0.05, Fig. 8E, F, G, H and I). It is noteworthy that the ratio of Bcl-2/Bax for the 20 and 60 mg/kg group was significantly increased compared to the 0 mg/kg group (p<0.05, Fig. 8J). We also evaluated in the same conditions expression of Fas, FasL and TNF-α, that were significantly increased at NP 60 (all p<0.05, Fig. 8K, L and M).

4. Discussion

Fertility can be evaluated by sperm concentration, motility and morphology [22]. Recently, it has been shown that NP has adverse effects on mammalian spermatogenesis [8, 23]. Moreover, NP can induce sperm toxicity as well as inhibit sperm motility *in vitro and in vivo* [7]. Under our experimental conditions, a direct relationship between excessive exposure to NP and the degree of deterioration in epididymal sperm parameters was observed. Importantly, high-dosage NP significantly caused an increase in incidence of sperm deformities. Our results suggest that the increases in NP treatment *in vivo* can impair epididymal sperm function and fertilizing capacity. Moreover, the histopathological analyses highlight seminiferous tubule degeneration after the higher-dose NP administration. These finding confirms other studies [15, 24] and further indicates that prepubertal exposure to excessive NP exposure inhibits the programming of spermatogenesis, thereby leading to spermatic damage and male reproductive disorders in pubertal-adolescent, and adult phase.

Spermatogenesis is dependent on a well-orchestrated hormonal environment [25]. Typically, LH and FSH are the primary tropic hormones that regulate testicular function [26]. LH and FSH secreted by the anterior pituitary can stimulate Sertoli and Leydig cells and, in turn, boost the secretion of testosterone from Leydig cells [27, 28]. In our study, although no significant change

in the testosterone serum levels, the serum LH and FSH levels at NP 60 mg/kg were considerably decreased, suggesting that NP induced hormonal imbalance. Fructose is the primary nutrient source for the sperm in the semen [29]. Low fructose concentration in the testis is related to low-sperm motility [30]. The diminished levels of testicular fructose observed here are in line with the suppression of sperm motility in the NP 60 mg/kg group. Altogether, we speculate that high exposure to NP could interfere with hypothalamus-pituitary-testicular axis that regulates Sertoli and Leydig cell function, through the production of hormone and fructose, thereby impairing spermatogenesis and affecting energy metabolism of sperm [31, 32].

The content of lipid peroxidation product and anti-oxidase activities can reflect the degree of OS [33]. In this study, the 60 mg/kg NP treatment resulted in a significant decrease GSH-Px and SOD activities with increasing MDA levels in testicular tissue and serum, indicating OS overwhelming the antioxidant defense system. Likewise, in the 60 mg/kg group, the decrease in testicular CAT, GPx1, SOD1 and CYP1B1 mRNA expression suggests spermatogenesis disorders that involve the compromised antioxidant capacities [34]. In general, testicular lipids are particularly susceptible to oxidative stress as they are relatively high (10-14%) in polyunsaturated fatty acids (PUFAs) [35]. PUFAs are an essential requirement for germ cells to maintain plasma membrane fluidity and normal physiological function of sperm [36]. Notably, owing to the pro-oxidant/antioxidant imbalance, reactive oxygen species attacks PUFAs in sperm cells and sperm plasma membrane leading to spermatozoa lipid peroxidation, which impairs sperm function [37]. In this regard, we speculate that NP-induced oxidative damage in the testis results in spermatogenic dysfunction.

Increasingly, evidence indicates that oxidative stress mediates apoptosis induced by chemical toxicity [17]. Apoptosis is a natural event that regulates germ cell turnover and maintains spermatogenesis; the immoderate apoptosis of spermatogenic cells would cause defective spermatogenesis leading to infertility [38]. PCNA, as a marker of cell proliferation, is expressed in spermatogonia and primary spermatocytes in all stages of the seminiferous tubules [39]. Our results demonstrated that higher dose of NP induced abnormal balance between cell proliferation and apoptosis, characterized by increased apoptotic germ cells and decreased PCNA-positive proliferating cells in seminiferous tubules. Furthermore, we observed that PCNA expression at mRNA and protein levels was downregulated at NP 60 mg/kg. Caspase signalling plays a pivotal role in the activation of apoptotic signal transmission and completion of apoptosis [40]. Specifically, caspase-3 converged with various death signals and has a key role in inducing apoptosis [41]. Cleaved-caspase-3 is one of the key executioners of apoptosis [42]. Our results revealed that NP activated caspase-3, identified by the production of cleaved-caspase-3. In this context, the oxidative stress-mediated caspase activation likely contributes to NP-induced testicular apoptosis.

The molecular mechanisms that promote caspase-mediated apoptosis are usually referred to the mitochondrial and death receptor pathways [43]. The Bcl-2/Bax signalling plays a central role in regulating the mitochondria-dependent apoptotic pathway for normal spermatogenesis in testis [38]. Significant changes in expression of Bcl-2 and Bax were observed in this study, including a decrease in the Bcl-2/Bax ratio, which confirmed that testicular cells accept signals to induce apoptosis [44]. The death receptor pathway, represented by the Fas/FasL system, has been reported to be involved in germ cell apoptosis [45]. The Fas-mediated apoptotic pathway consists

of several steps that involve the caspase family; in particular, the activation of Fas/FasL signalling can drive apoptosis via caspase-3 [46]. Moreover, the induction of Fas/FasL-driven apoptosis that modulated by TNF-α and IFN-γ stimulates the release of pro-inflammatory IL-1β [47]. Herein, we demonstrate that the mRNA and protein expression of Fas, FasL and TNF-α visibly changed at NP 60 mg/kg, while the mRNA levels of IL-1β and IFN-γ were significantly elevated. Accordingly, Fas/FasL-induced signalling possibly governs both the functional activation of caspase and the subsequent germ cell apoptosis associated with the testicular toxicity induced by NP.

Accumulation of p53 is important in the cellular emergency response to OS [48]. Once activated by OS, p53 transcriptionally triggers the activation of pro-apoptotic Bax and the constitutive Bcl-2/Bcl-xL inhibition [49]. The release of cytochrome *c*, regulated by Bcl-2 family members, is the switch to turn on/off apoptosis [50]. To nucleate apoptosome formation, cytosolic cytochrome *c* binds the adaptor protein Apaf-1, accelerating the activation caspases cascade-dependent apoptosis [49]. In agreement with this theory, our study showed that p53, cytochrome *c* and Apaf-1was upregulated after 60 mg/kg NP treatment at both mRNA and protein levels. Induction of active p53 appears to promote the convergence of the intrinsic and extrinsic signalling pathways at the mitochondrial level [51]. Recent research has revealed new aspects showing that intracellular OS may not have efficient machinery to activate the intrinsic pathway completely and may have to stimulate the extrinsic apoptotic pathway to trigger full caspase activation [52, 53]. The cross-talk between these pathways allows caspase-driven signal amplification to ensure sufficient removal of damaged cells in testis [51]. Here we suggest that Fas/FasL signalling may collaborate in p53-mitochondrial apoptotic program, leading to apoptosis in testicular germ cells. Nonetheless, the precise molecular mechanisms involved in the joint regulation of p53-dependent intrinsic and extrinsic apoptosis induced by NP are not yet clear.

Hormetic effects on organisms are considered an adaptive response to a moderate stress induced by the stimulus [54]. In this study, the most fascinating finding is the stimulatory effect of the 5 mg/kg NP treatment on epididymal sperm production, motility and sperm quality. Moreover, that active mature and fully functioning seminiferous tubules were observed at NP 5 mg/kg using histopathological techniques. These observations support the concept that NP stimulates a response from the testis structure and sperm parameters at low concentrations. Hormesis is characterized by stimulatory effects at low dose and inhibitory effects at higher concentrations [55, 56]. In this respect, our results suggest that NP induces hormetic-like biphasic dose-response relationships in testis. Hormetic dose responses represent an overcompensation due to a disruption to the homeostasis based biological feedback system [57].Therefore it is not unexpected that such hormetic-like biphasic dose responses following moderate NP exposure is the induction of adaptive tolerance.

To understand this further, there is a need to clarify the mechanistic foundations of NP-induced hormesis. In our study, 5 mg/kg NP not only markedly suppressed caspase-1, -3, -6, -9 and Apaf-1 activation at the mRNA level, but also produced a significant increase in the mRNA expression of PCNA1, with respect to the control group. Disappointingly, we did not find any other association for any of the other tested proteins. This implies that another distinct signalling pathway is activated in response to this level of exposure, which poses the question to what type of mechanism may contribute to such hormetic or adaptive response to NP treatment. Receptor-mediated and cell signalling-mediated bidirectional control of gene expression has been

considered as the main hormetic mechanism triggered by exposure to chemicals [58]. It is reported that hormesis likely depends upon changes in the regulation of genes critical for OS resistance [55, 59]. Furthermore, Scott et al suggested that the hormetic effect may be attributed to rapid up-regulation of the adaptive-response genes [60]. In this context, hormetic responses driven by Apaf-1/caspase genes- induced by NP, is probably involved in spermatogenesis and sperm quality. This is under the assumption that Apaf-1-mediated caspase activation is important for the regulation of germ cell proliferation and differentiation in testis. In our next study, we will perform specific experiments designed to address this hypothesis.

5. Conclusions

In summary, our study is the first to report that NP induced hormetic dose responses, in which low dose NP stimulated spermatogenesis and augmented epididymal sperm parameters in prepubertal rats, in contrast, NP at higher dose causes adverse effects such as hormone deficiency, disorders of fructose metabolism and testicular oxidative damage, consequently inhibiting cell proliferation, impairing testicular functions and compromising sperm function. In addition, NP induces testicular germ cell apoptosis by the possible mechanisms of both extrinsic-mediated and intrinsic-mediated pathways *in vivo*. These findings contribute to understanding the mechanism of NP on male fertility. Further studies are required to examine the molecular pathways that are involved in the alterations described herein.

Conflict of Interest

The authors declare no competing financial interests.

Transparency document

The Transparency document associated with this article can be found in the online version.

Acknowledgment

This work is supported by grants from The National Natural Science Foundation of China (grant number: 81372960，81172623).

References

[1] Zhang HY, Xue WY, Li YY, et al. Perinatal exposure to 4-nonylphenol affects adipogenesis in first and second generation rats offspring. Toxicol Lett 2014;225(2):325-32.
[2] Jin X, Wang Y, Jin W, et al. Ecological risk of nonylphenol in China surface waters based on reproductive fitness. Environ Sci Technol 2014;48(2):1256-62.
[3] Niu Y, Zhang J, Duan H, Wu Y, Shao B. Bisphenol A and nonylphenol in foodstuffs: Chinese dietary exposure from the 2007 total diet study and infant health risk from formulas. Food Chem 2015;167:320-5.
[4] Directive 2008/105/EC of the European Parliament and of the Council on environmental quality standards in the field of water policy. Official Journal of the European Union 2008.
[5] Roig B, Cadiere A, Bressieux S, Biau S, Faure S, de Santa Barbara P. Environmental concentration of nonylphenol alters the development of urogenital and visceral organs in avian model. Environ Int 2014;62:78-85.
[6] Chen M, Tang R, Fu G, et al. Association of exposure to phenols and idiopathic male infertility. J Hazard Mater 2013;250-251:115-21.
[7] Lukac N, Lukacova J, Pinto B, Knazicka Z, Tvrda E, Massanyi P. The effect of nonylphenol on the motility and viability of bovine spermatozoa in vitro. J Environ Sci Health A Tox Hazard Subst Environ Eng 2013;48(8):973-9.
[8] Uguz C, Varisli O, Agca C, Evans T, Agca Y. In vitro effects of nonylphenol on motility, mitochondrial, acrosomal and chromatin integrity of ram and boar spermatozoa. Andrologia 2015;47(8):910-9.
[9] Uguz C, Varisli O, Agca C, Agca Y. Effects of nonylphenol on motility and subcellular elements of epididymal rat sperm. Reprod Toxicol 2009;28(4):542-9.
[10] Aly HA, Domenech O, Banjar ZM. Effect of nonylphenol on male reproduction: analysis of rat epididymal biochemical markers and antioxidant defense enzymes. Toxicol Appl Pharmacol 2012;261(2):134-41.
[11] Moody S, Goh H, Bielanowicz A, Rippon P, Loveland KL, Itman C. Prepubertal mouse testis growth and maturation and androgen production are acutely sensitive to di-n-butyl phthalate. Endocrinology 2013;154(9):3460-75.
[12] Stoker TE, Parks LG, Gray LE, Cooper RL. Endocrine-disrupting chemicals: prepubertal exposures and effects on sexual maturation and thyroid function in the male rat. A focus on the EDSTAC recommendations. Endocrine Disrupter Screening and Testing Advisory Committee. Crit Rev Toxicol 2000;30(2):197-252.
[13] Erkekoglu P, Zeybek ND, Giray B, Asan E, Hincal F. The effects of di(2-ethylhexyl)phthalate exposure and selenium nutrition on sertoli cell vimentin structure and germ-cell apoptosis in rat testis. Arch Environ Contam Toxicol 2012;62(3):539-47.
[14] Zhao YM, Gao LP, Zhang HL, Guo JX, Guo PP. Grape seed proanthocyanidin extract prevents DDP-induced testicular toxicity in rats. Food Funct 2014;5(3):605-11.
[15] Lu WC, Wang AQ, Chen XL, et al. 90d Exposure to Nonylphenol has Adverse Effects on the Spermatogenesis and Sperm Maturation of Adult Male Rats. Biomed Environ Sci 2014;27(11):907-11.
[16] Chitra KC, Latchoumycandane C, Mathur PP. Effect of nonylphenol on the antioxidant system in epididymal sperm of rats. Arch Toxicol 2002;76(9):545-51.
[17] Figarola JL, Singhal J, Rahbar S, Awasthi S, Singhal SS. LR-90 prevents

methylglyoxal-induced oxidative stress and apoptosis in human endothelial cells. Apoptosis 2014;19(5):776-88.

[18] Durairajanayagam D, Agarwal A, Ong C. Causes, effects and molecular mechanisms of testicular heat stress. Reprod Biomed Online 2015;30(1):14-27.

[19] Yu G, Guo Q, Xie L, Liu Y, Wang X. Effects of subchronic exposure to carbendazim on spermatogenesis and fertility in male rats. Toxicol Ind Health 2009;25(1):41-7.

[20] Quan C, Shi Y, Wang C, Wang C, Yang K. p,p'-DDE damages spermatogenesis via phospholipid hydroperoxide glutathione peroxidase depletion and mitochondria apoptosis pathway. Environ Toxicol. 2014.

[21] Wang C, Fu W, Quan C, et al. The role of Pten/Akt signaling pathway involved in BPA-induced apoptosis of rat Sertoli cells. Environ Toxicol 2015;30(7):793-802.

[22] Buck Louis GM, Sundaram R, Schisterman EF, et al. Semen quality and time to pregnancy: the Longitudinal Investigation of Fertility and the Environment Study. Fertil Steril 2014;101(2):453-62.

[23] Han XD, Tu ZG, Gong Y, et al. The toxic effects of nonylphenol on the reproductive system of male rats. Reprod Toxicol 2004;19(2):215-21.

[24] McClusky LM, Patrick S, Barnhoorn IE, van Dyk JC, de Jager C, Bornman MS. Immunohistochemical study of nuclear changes associated with male germ cell death and spermiogenesis. J Mol Histol 2009;40(4):287-99.

[25] Wisniewski P, Romano RM, Kizys MM, et al. Adult exposure to bisphenol A (BPA) in Wistar rats reduces sperm quality with disruption of the hypothalamic-pituitary-testicular axis. Toxicology 2015;329:1-9.

[26] Li E, Guo Y, Wang G, Chen F, Li Q. Effect of resveratrol on restoring spermatogenesis in experimental cryptorchid mice and analysis of related differentially expressed proteins. Cell Biol Int 2015;39(6):733-40.

[27] Yin HP, Xu JP, Zhou XQ, Wang Y. Effects of vitamin E on reproductive hormones and testis structure in chronic dioxin-treated mice. Toxicol Ind Health 2012;28(2):152-61.

[28] Wu JJ, Wang KL, Wang SW, et al. Differential effects of nonylphenol on testosterone secretion in rat Leydig cells. Toxicology 2010;268(1-2):1-7.

[29] Yefimova MG, Messaddeq N, Harnois T, et al. A chimerical phagocytosis model reveals the recruitment by Sertoli cells of autophagy for the degradation of ingested illegitimate substrates. Autophagy 2013;9(5):653-66.

[30] Breikaa RM, Mosli HA, Nagy AA, Abdel-Naim AB. Adverse testicular effects of Botox(R) in mature rats. Toxicol Appl Pharmacol 2014;275(2):182-8.

[31] Ahmad MK, Mahdi AA, Shukla KK, et al. Withania somnifera improves semen quality by regulating reproductive hormone levels and oxidative stress in seminal plasma of infertile males. Fertil Steril 2010;94(3):989-96.

[32] Shono T, Taguchi T. Short-time exposure to mono-n-butyl phthalate (MBP)-induced oxidative stress associated with DNA damage and the atrophy of the testis in pubertal rats. Environ Sci Pollut Res Int 2014;21(4):3187-90.

[33] Gong Y, Wu J, Huang Y, Shen S, Han X. Nonylphenol induces apoptosis in rat testicular Sertoli cells via endoplasmic reticulum stress. Toxicol Lett 2009;186(2):84-95.

[34] Zhao J, Zhai L, Liu Z, Wu S, Xu L. Leptin level and oxidative stress contribute to obesity-induced low testosterone in murine testicular tissue. Oxid Med Cell Longev

2014;2014:190945.
[35] Nair N. Dose-dependent short-term study of di-n-butyl phthalate on the testicular antioxidant system of Wistar rats. Environ Sci Pollut Res Int 2015;22(3):2196-204.
[36] Said L, Banni M, Kerkeni A, Said K, Messaoudi I. Influence of combined treatment with zinc and selenium on cadmium induced testicular pathophysiology in rat. Food Chem Toxicol 2010;48(10):2759-65.
[37] Wright C, Milne S, Leeson H. Sperm DNA damage caused by oxidative stress: modifiable clinical, lifestyle and nutritional factors in male infertility. Reprod Biomed Online 2014;28(6):684-703.
[38] Eleawa SM, Alkhateeb MA, Alhashem FH, et al. Resveratrol reverses cadmium chloride-induced testicular damage and subfertility by downregulating p53 and Bax and upregulating gonadotropins and Bcl-2 gene expression. J Reprod Dev 2014;60(2):115-27.
[39] Kanter M. Thymoquinone reestablishes spermatogenesis after testicular injury caused by chronic toluene exposure in rats. Toxicol Ind Health 2011;27(2):155-66.
[40] Peng X, Zhang YY, Wang J, Ji Q. Ethylacetate extract from Tetrastigma hemsleyanum induces apoptosis via the mitochondrial caspase-dependent intrinsic pathway in HepG cells. Tumour Biol 2015.
[41] Liu C, Duan W, Li R, et al. Exposure to bisphenol A disrupts meiotic progression during spermatogenesis in adult rats through estrogen-like activity. Cell Death Dis 2013;4:1-10.
[42] Jung EB, Lee CS. Baicalein attenuates proteasome inhibition-induced apoptosis by suppressing the activation of the mitochondrial pathway and the caspase-8- and Bid-dependent pathways. Eur J Pharmacol 2014;730:116-24.
[43] Ahn JH, Lee TW, Kim KH, et al. 6-Acetoxy Cyperene, a Patchoulane-type Sesquiterpene Isolated from Cyperus rotundus Rhizomes Induces Caspase-dependent Apoptosis in Human Ovarian Cancer Cells. Phytother Res 2015; 29(9):1330-8.
[44] Luo Q, Li J, Cui X, Yan J, Zhao Q, Xiang C. The effect of Lycium barbarum polysaccharides on the male rats reproductive system and spermatogenic cell apoptosis exposed to low-dose ionizing irradiation. J Ethnopharmacol 2014;154(1):249-58.
[45] Zhao XF, Wang Q, Ji YL, et al. Fenvalerate induces germ cell apoptosis in mouse testes through the Fas/FasL signaling pathway. Arch Toxicol 2011;85(9):1101-8.
[46] Croker BA, O'Donnell JA, Nowell CJ, et al. Fas-mediated neutrophil apoptosis is accelerated by Bid, Bak, and Bax and inhibited by Bcl-2 and Mcl-1. Proc Natl Acad Sci U S A 2011;108(32):13135-40.
[47] Bossaller L, Chiang PI, Schmidt-Lauber C, et al. Cutting edge: FAS (CD95) mediates noncanonical IL-1beta and IL-18 maturation via caspase-8 in an RIP3-independent manner. J Immunol 2012;189(12):5508-12.
[48] Yin Y, Chen W, Tang C, et al. NF-kappaB, JNK and p53 pathways are involved in tubeimoside-1-induced apoptosis in HepG2 cells with oxidative stress and G(2)/M cell cycle arrest. Food Chem Toxicol 2011;49(12):3046-54.
[49] Sarkar R, Mukherjee S, Biswas J, Roy M. Sulphoraphane, a naturally occurring isothiocyanate induces apoptosis in breast cancer cells by targeting heat shock proteins. Biochem Biophys Res Commun 2012;427(1):80-5.
[50] Sukhotnik I, Nativ O, Roitburt A, et al. Methotrexate induces germ cell apoptosis and impairs spermatogenesis in a rat. Pediatr Surg Int 2013;29(2):179-84.

[51] Sawant PB, Bera A, Dasgupta S, Sawant BT, Chadha NK, Pal AK. p53 dependent apoptotic cell death induces embryonic malformation in Carassius auratus under chronic hypoxia. PLoS One 2014;9(7):e102650.
[52] Liu Y, Borchert GL, Surazynski A, Hu CA, Phang JM. Proline oxidase activates both intrinsic and extrinsic pathways for apoptosis: the role of ROS/superoxides, NFAT and MEK/ERK signaling. Oncogene 2006;25(41):5640-7.
[53] McIlwain DR, Berger T, Mak TW. Caspase functions in cell death and disease. Cold Spring Harb Perspect Biol 2015;7(4):1-28.
[54] Bao J, Huang B, Zou L, et al. Hormetic Effect of Berberine Attenuates the Anticancer Activity of Chemotherapeutic Agents. PLoS One 2015;10(9):e0139298.
[55] Calabrese EJ. Hormetic mechanisms. Crit Rev Toxicol 2013;43(7):580-606.
[56] Marnef A, Jady BE, Kiss T. Human polypyrimidine tract-binding protein interacts with mitochondrial tRNAThr in the cytosol. Nucleic Acids Res 2016;44(3):1342-53.
[57] Calabrese EJ, Baldwin LA. Hormesis: U-shaped dose responses and their centrality in toxicology. Trends in Pharmacological Sciences 2001;22(6):285-91.
[58] Chen F, Liu SS, Yu M, Qu R, Wang MC. Blocking the entrance of AMP pocket results in hormetic stimulation of imidazolium-based ionic liquids to firefly luciferase. Chemosphere 2015;132:108-13.
[59] Cypser JR, Johnson TE. Multiple stressors in Caenorhabditis elegans induce stress hormesis and extended longevity. J Gerontol A Biol Sci Med Sci 2002;57(3):B109-14.
[60] Scott BR, Belinsky SA, Leng S, Lin Y, Wilder JA, Damiani LA. Radiation-stimulated epigenetic reprogramming of adaptive-response genes in the lung: an evolutionary gift for mounting adaptive protection against lung cancer. Dose Response 2009;7(2):104-31.

Figure captions

Fig.1. Effects of 4-nonylphenol on epididymal sperm morphology in rats. Major morphological changes in spermatozoa: White arrowheads, normal form; Yellow arrowheads, coiled and bent tail; Black arrowhead, tailless form; Red arrowheads, double head; Pink arrowhead, pin head; Blue arrowhead, big head. Magnification: ×200.

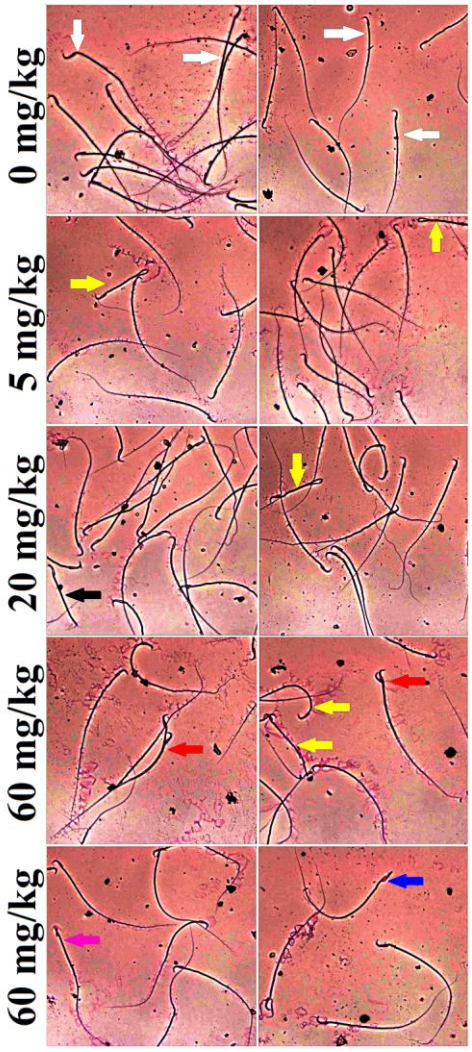

Fig.2. 4-nonylphenol exposure affected the serum hormone and fructose content in testis. Each bar denotes Mean ± S.D. of six rats. *P <0.05, **P <0.01 versus the 0 mg/kg group, one-way ANOVA.

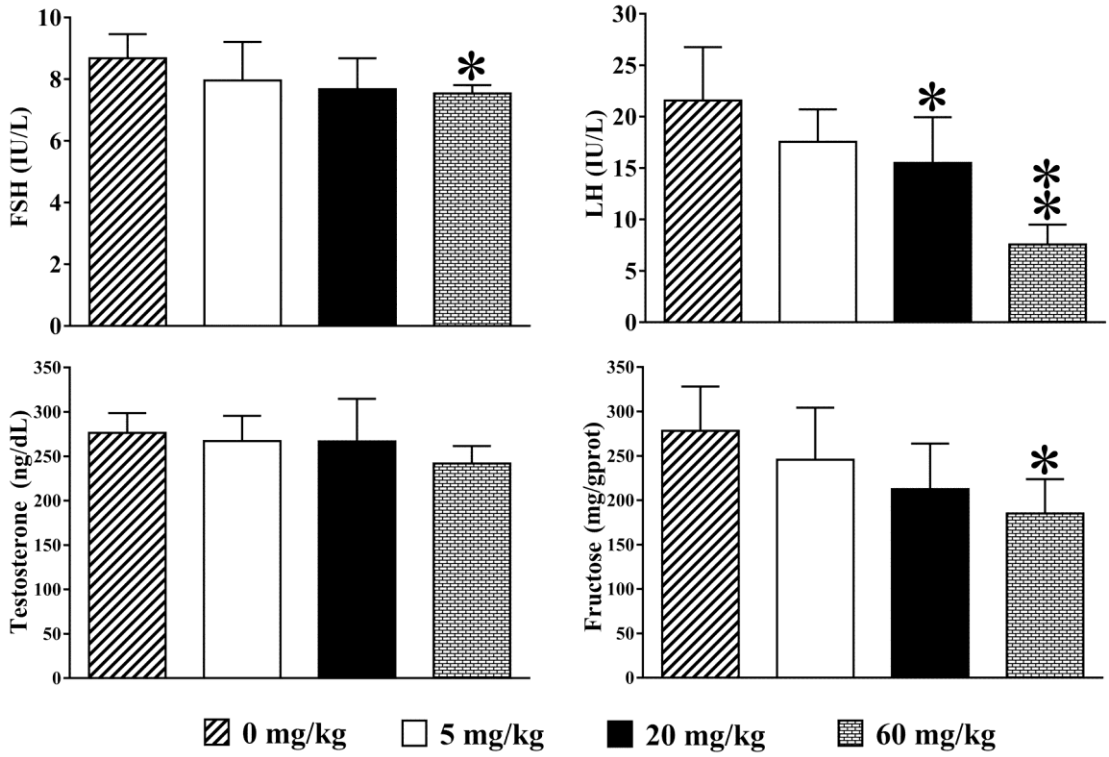

Fig.3. Histological morphology of testis stained with H&E from the 4-nonylphenol-treated and the control groups. (A) Histological cross-sections of seminiferous tubules and spermatogenesis appeared normal in the 0 mg/kg group. (B) In the 5 mg/kg 4-nonylphenol group, most of the tubule walls were smooth, and the arrangement of the seminiferous tubule was regular; (C) The spermatocyte detached and irregularly lined, and the arrangement of the seminiferous tubule was distorted at 4-nonylphenol 20 mg/kg; (D) After 60 mg/kg 4-nonylphenol administration, spermatozoas in the tubules reduced as compared with the control group, and the germ cell layers of the seminiferous tubules were discontinuous, even some sloughed germ cells detached into the tubular lumen. Magnification: ×200.

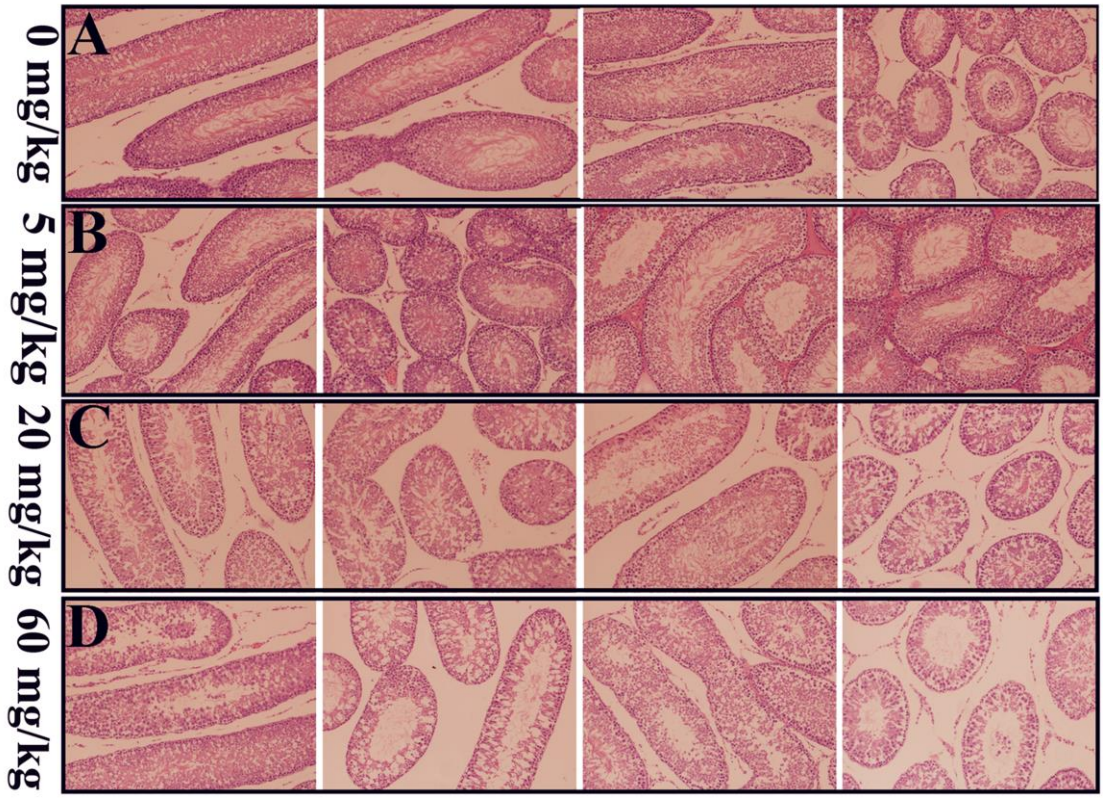

Fig.4. Effects of 4-nonylphenol at different doses on oxidative stress in rats. (A) Effect of 4-nonylphenol on SOD, GSH-Px and MDA of testicular tissue in rats. (B) Effect of 4-nonylphenol on the levels of serum SOD, GSH-Px and MDA in rats. Each bar denotes Mean ± S.D. of six rats. **P* <0.05, ***P* <0.01 versus group without 4-nonylphenol treatment, one-way ANOVA.

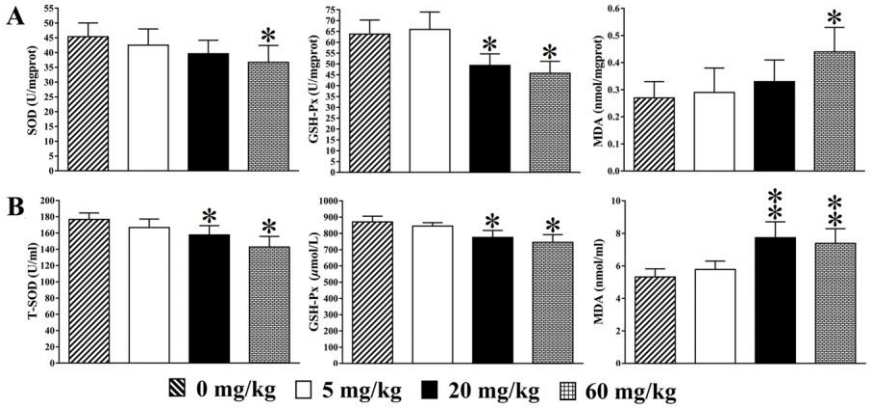

Fig.5. Effects of different-dose 4-nonylphenol on mRNA levels of SOD1, CAT, GPx1 and CYP1B1 in rat testis. Each bar denotes Mean ± S.D. of six rats. **P* <0.05, ***P* <0.01 versus group without 4-nonylphenol treatment, one-way ANOVA.

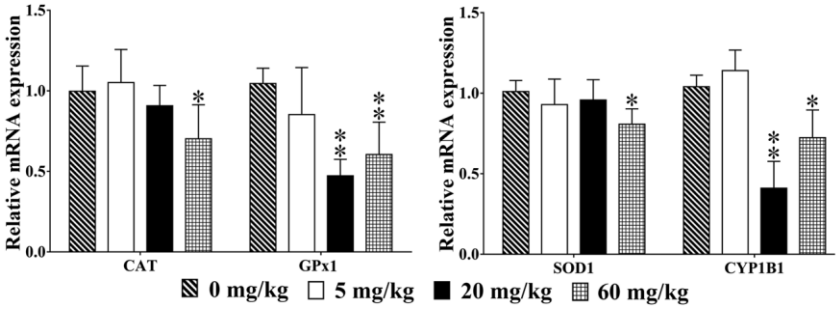

Fig.6. Testicular apoptosis was induced by 4-nonylphenol. (A) Electron micrographs of testicular tissue in different groups. Seminiferous epithelium from the 0 mg/kg 4-nonylphenol group rats showing normal spermatogonia with homogeneous chromatin; In the 5 mg/kg group, the morphology of organelles was normal without obvious alteration; In the 20 mg/kg group, swollen mitochondria, widened endoplasmic reticulum, big vacuolar spaces, increased lipid droplets and heterochromatic nucleus could be seen; In the 60 mg/kg group, showing primary spermatocytes with irregular, damaged nuclear membrane, cytoplasmic vacuoles, and damaged mitochondria. Bar: 2 μm. Three rats were randomly selected from each treatment group for ultrastructure evaluation. (B) Effects of 4-nonylphenol on TUNEL-positive apoptotic changes in seminiferous tubules of rats. TUNEL-positive staining indicative of DNA fragmentation was detected as bright-green fluorescent on the nuclei of apoptotic cells. Magnification: ×200.

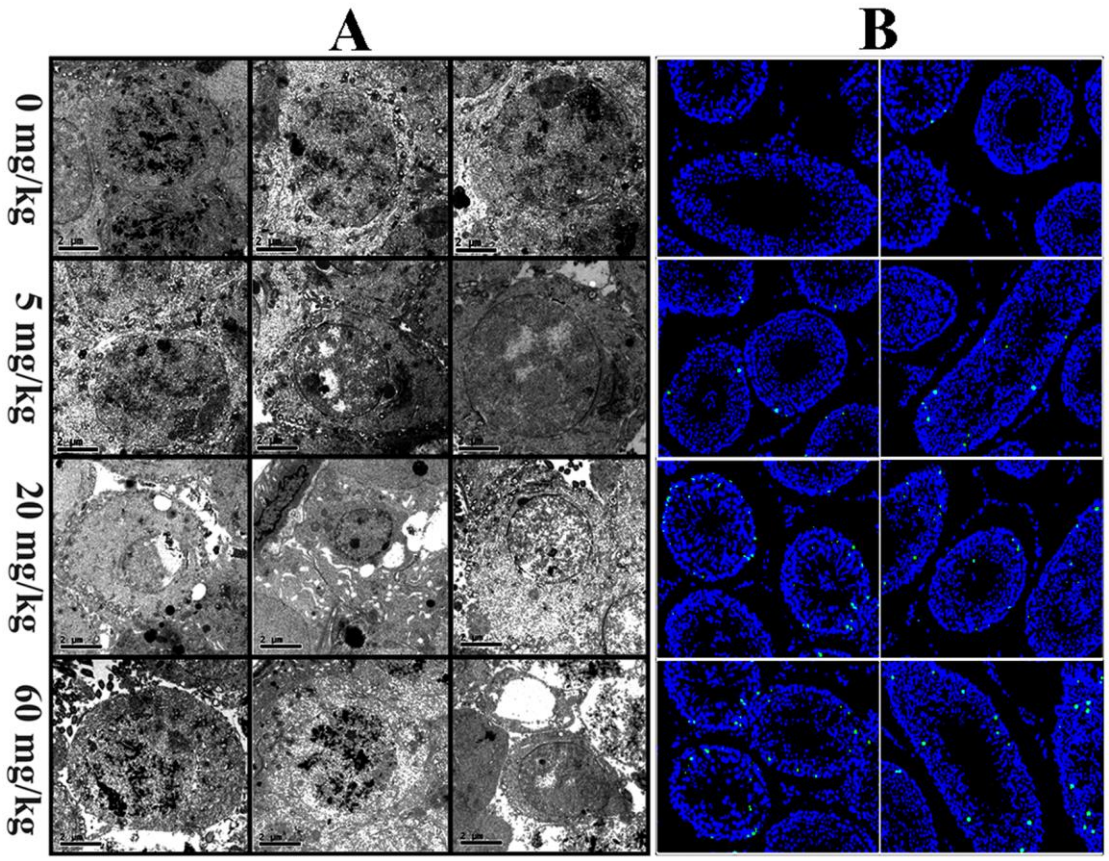

Fig.7. Effects of 4-nonylphenol at different doses on the expression of PCNA and p53 in rat testis. (A) Testis immunohistochemically stained for PCNA. PCNA-positive (PCNA+) and -negative (PCNA-) cells were stained in dark and light blue, respectively. Red arrowheads: PCNA+ cell; Black arrowhead: PCNA- cell. In the 0 mg/kg and 5 mg/kg groups, PCNA+ cells were strongly detected in spermatogonia and spermatocytes. PCNA+ cells were obviously decreased in the 20 mg/kg group compared with the 0 mg/kg group. PCNA activity was significantly lower in secondary spermatocytes and early-stage sperm cells at 4-nonylphenol 60 mg/kg. (B) Immunofluorescence study showing p53 activation in rat seminiferous tubules. p53 expression was mainly localised to the early stage sperm cells in seminiferous tubules as indicated by red arrowheads. There is a much greater distribution of p53-expressing nuclei in seminiferous tubules of the 20 mg/kg and 60 mg/kg groups than the 0 mg/kg group. Magnification: ×200

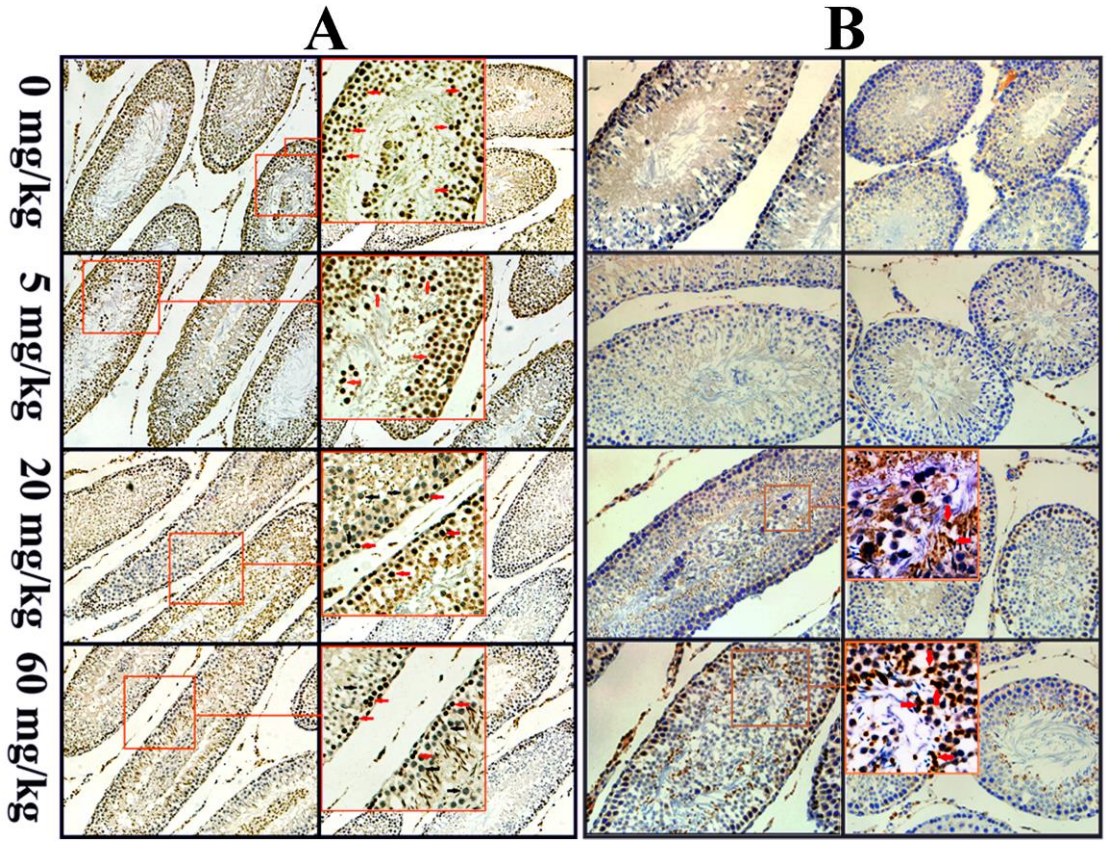

Fig.8. 4-nonylphenol induced testicular toxicity involving the activation of p53-Bcl-2/Bax-Fas signalling pathways. (A) 4-nonylphenol regulated the expressions of proteins related to cell proliferation and apoptosis. Equal loading of protein was confirmed by stripping the immunoblot and reprobing it for β-actin. The immunoblots shown here are representative of three independent western blot experiments. Densitometry analyses of the effect of NP on the target protein levels are represented for Bcl-2 (B), PCNA (C), pro-caspase-3 (D), p53 (E), bax (F), Apaf-1 (G), cytochrome *c* (H), cleaved-caspase-3 (I), Bcl-2/bax (J), Fas (K), FasL (L) and TNF-α (M). Quantitative data are expressed as mean ± SD. n = 6. The Y axis represents the relative protein expression level (the ratio of target protein/β-actin and Bcl-2/bax). * $P < 0.05$, ** $P < 0.01$ versus control group without NP treatment, one-way ANOVA.

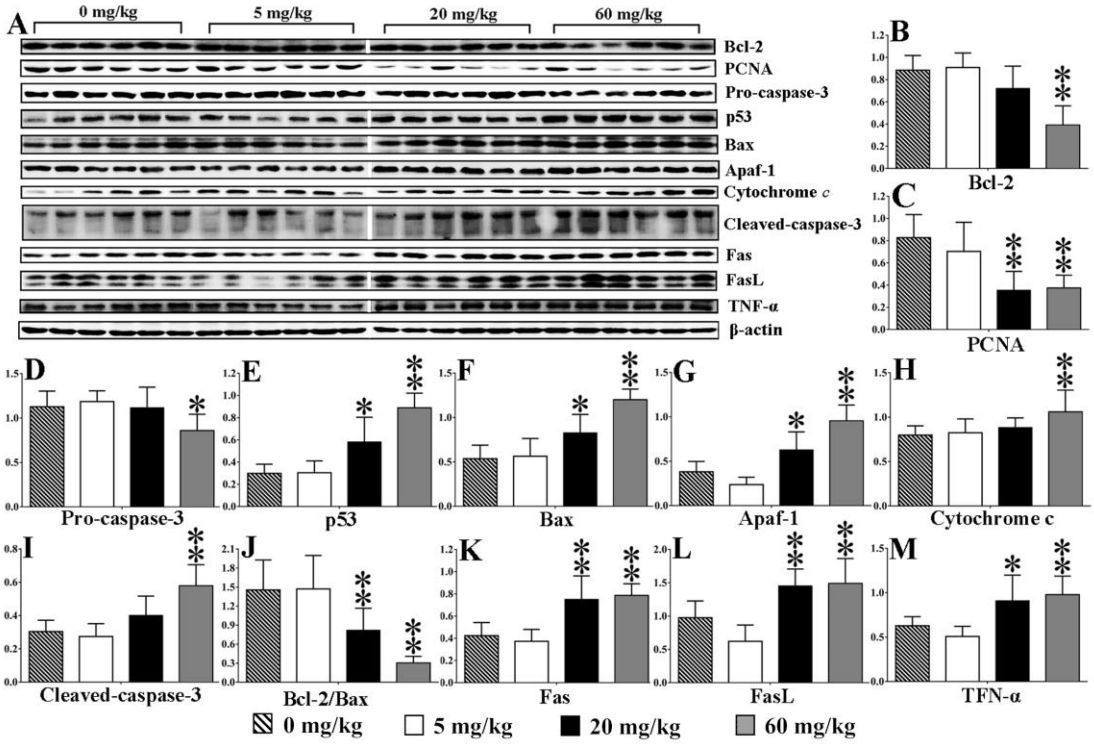

Table 1 Effect of 4-nonylphenol at different doses on sperm concentration, motility, motility parameters and morphology

Parameters	4-nonylphenol (mg/kg body weight every 2 days)			
	0	5	20	60
Sperm density and motility				
Total counts	470.33±166.44	727.67±143.06*	409.50±125.31	278.67±79.20*
Total motility	229.17±116.46	351.33±82.00**	217.83±55.78	123.17±38.83**
Total density (millions/mL)	28.96±4.66	39.99±4.89*	23.57±7.29	19.82±4.52
Activate rate (%)	45.40±9.48	45.80±5.44	51.70±11.65	41.49±2.62
Motile sperm density (millions/mL)	12.18±1.93	18.96±1.80**	12.82±1.84	9.85±1.55*
Motion parameters				
VCL (μm/s)	35.92±4.83	40.11±7.51	39.41±3.52	31.47±8.62
VSL (μm/s)	18.70±3.46	21.81±7.08	17.78±5.58	16.83±5.35
VAP (μm/s)	22.74±3.61	26.04±7.17	22.30±5.14	20.30±5.51
Average ALH (μm)	4.95±0.65	5.22±0.77	5.29±0.64	4.21±1.17
Maximal ALH (μm)	12.39±0.98	13.66±1.49	12.75±1.54	10.68±2.47
Average BCF (times/s)	9.54±1.05	9.26±0.98	10.35±1.47	8.46±2.24
Rates of FP (%)	23.42±3.61	25.01±7.20	22.07±8.13	22.50±6.55
Density of FP (millions/mL)	6.52±1.66	9.89±2.15*	5.09±1.26	3.71±1.14*
Sperm swimming velocity				
Sperms of grade A (%)	8.87±2.02	15.97±3.37**	7.90±2.24	8.85±2.87
Sperms of grade B (%)	10.58±3.23	9.21±2.16	10.60±2.61	8.54±1.96
Sperms of grade C (%)	25.96±5.36	20.62±3.09	36.94±10.81**	24.68±4.04
Sperms of grade D (%)	54.60±9.48	54.42±2.22	44.56±8.79*	57.93±7.18
Sperms of grade A&B (%)	19.45±5.02	25.18±4.56*	18.50±4.53	17.39±4.54
Sperms of grade C&D (%)	80.55±5.02	74.82±6.31	81.09±6.20	83.02±9.03
Sperm morphology				
Total abnormalities (%)	5.08±1.82	6.88±1.24	9.46±1.78*	12.29±3.04**

Note: The control data are within the range of normal historical control data in our laboratory. Mean ± SD, n=6 for each treatment group. *P <0.05, **P <0.01 versus 0 mg/kg group, one-way ANOVA. Curvilinear velocity (VCL); Straight line velocity (VSL); Average path velocity (VAP); Amplitude of lateral head displacement (ALH); Beat cross frequency (BCF); Sperm moving in forward linear motion called forward progression (FP).

Table 2 Effects of 4-nonylphenol on mRNA levels of proliferation- and apoptosis-related genes of testicular tissue in rats

Gene	4-nonylphenol (mg/kg body weight every 2 days)			
	0	5	20	60
Proliferation marker				
PCNA1	1.060±0.059	1.552±0.381**	0.306±0.131**	0.643±0.189**
Caspase family				
Caspase 1	1.062±0.129	0.645±0.192*	1.102±0.388[a]	1.362±0.376
Caspase 3	1.018±0.116	0.690±0.187**	0.770±0.148*	1.223±0.177*
Caspase 6	1.022±0.051	0.820±0.176*	1.033±0.165	0.991±0.171
Caspase 7	1.008±0.056	1.067±0.062	0.491±0.093**	0.722±0.101**
Caspase 8	1.036±0.129	0.850±0.154	1.126±0.318	1.076±0.262
Caspase 9	1.060±0.104	0.659±0.148*	0.723±0.247*	1.243±0.374
Caspase 11	1.057±0.138	0.914±0.187	1.188±0.286	1.219±0.125
Bcl-2 family				
Bad	1.019±0.108	1.101±0.063	0.994±0.139	1.016±0.069
Bax	1.022±0.064	0.843±0.137	1.123±0.218	1.372±0.226*
Bcl-2	1.011±0.186	1.047±0.089	0.681±0.238*	0.867±0.177
Bcl-xl	1.008±0.257	1.007±0.108	0.582±0.112*	0.749±0.267
p53-mediated mitochondrial signal				
Cytochrome c	0.993±0.163	1.011±0.149	1.276±0.284*	1.307±0.257*
Apaf-1	1.146±0.223	0.858±0.111*	1.208±0.307	1.807±0.189**
p53	1.005±0.075	1.083±0.143	0.927±0.193	1.285±0.187**
Death receptor apoptotic signal				
Fas	1.007±0.094	1.857±0.508**	1.958±0.501**	2.024±0.550**
FasL	0.999±0.088	1.427±0.252*	1.838±0.449**	1.656±0.368**
IL-1β	1.081±0.137	1.597±0.328**	0.400±0.103**	0.693±0.175**
TNF-a	1.078±0.075	1.387±0.148	1.435±0.336	1.986±0.519**
IFN-γ	1.001±0.145	0.537±0.136*	1.369±0.394	1.336±0.427

Note: The data are expressed as the mean ± SD for six animals per dose. *P <0.05, **P <0.01 versus 0 mg/kg group, one-way ANOVA.